Chapter 5
Monitoring of Hybrid Dynamic Systems: Application to Chemical Process

Nelly Olivier-Maget and Gilles Hetreux

5.1 Introduction

In this chapter, a methodology of a fault detection and isolation for chemical process is presented. This methodology, called SimAEM (Simulation Abnormal Event Management) is particularly designed for the monitoring of batch and semi-continuous processes. These processes are the prevalent production mode for low volume of high added value products. Such processes are composed of interconnected and shared resources, in which a continuous treatment is carried out. For this reason, they are generally considered as hybrid systems where discrete aspects mix with continuous ones. Otherwise, the recipe is more often described with state events (temperature or composition threshold, etc.) than with fixed processing times [1]. SimAEM methodology is a model-based approach. Model-based diagnosis is widely discussed in the literature and many industrial applications exploit this principle [2]. Most of the methods in this approach are designed in three stages: residual generation, residual assessment and localization. In our study, our approach is based on a hybrid dynamic simulator. This simulator provides a reference model, which is supposed to be correct [3, 26]. The general architecture of SimAEM monitoring system is shown in Fig. 5.1.

The sequence of the different steps of a failure diagnosis is highlighted. Moreover, a distinction between the on-line and off-line steps is made. Our approach is therefore divided into three steps:

N. Olivier-Maget (✉) · G. Hetreux
Laboratoire de Génie Chimique, Université de Toulouse, CNRS, Toulouse, France
e-mail: nelly.olivier@ensiacet.fr

M. Sayed-Mouchaweh (ed.), *Fault Diagnosis of Hybrid Dynamic and Complex Systems*, https://doi.org/10.1007/978-3-319-74014-0_5

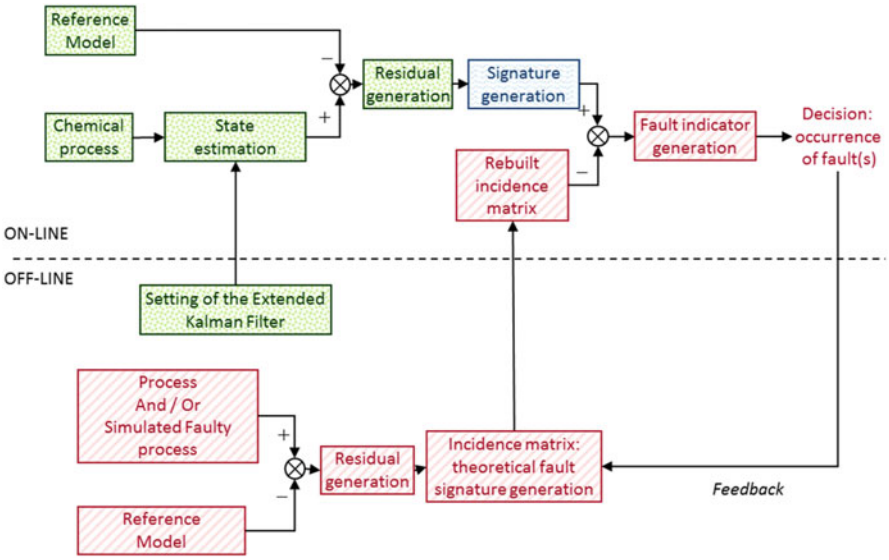

Fig. 5.1 SimAEM architecture

- The first step is the residual generation (in dotted motif in Fig. 5.1). It consists of the comparison between the predicted model obtained by simulation and the real system behaviour obtained by an observer. In our case, the extended Kalman filter is implemented. The aim is to reconstruct the system outputs from measurements.
- The second step (the signature generation) aims to analyse the residuals (in wave motif in Fig. 5.1). This is the detection step. It determines the presence or absence of a failure. The "signature" notion is introduced.
- Finally, the last step (in hatched motif in Fig. 5.1) consists of fault diagnosis. This step exploits the generated signatures in the previous step in order to determine the fault type. To do this, an inline matching process has been made. This is a pattern recognition problem. For this purpose, the instantaneous fault signature is then compared with the theoretical fault signatures by the calculation of distances in order to identify and localize the fault(s). These theoretical fault signatures are listed in the incidence table. The latter is obtained by experiment or by the off-line simulation of a faulty process.

5.2 Residual Generation by the Extended Kalman Filter

The initial step of a model-based diagnosis system generates fault indicators, called residuals. The residuals contain information on the drift or failure of the monitored system. The goal is to measure the difference between the system measurements

and the so-called "theoretical" value obtained by a reference model. The generation of residual is a critical step in the success of the diagnosis.

5.2.1 State Estimator: Extended Kalman Filter

Numerous works on Hybrid Dynamic Systems revolve around the axes of modelling, stability and controllability [4]. In recent years, more particular efforts have been made in the literature on observability. The high robustness and real-time ability of observer is well-known for industrial applications [5]. Although the theory of state observation has reached a certain degree of maturity in the domains of continuous and discrete events, the observation of dynamic hybrid systems remain a challenge.

The observation of state is particularly adapted to the studies of fault detection and diagnosis. It provides more information to make decision. Thus, the residual generation by a state estimation consists of rebuilding the state or, more generally, the process output by using observers, and then using the error estimation as residual. Clark was one of the first to use this concept [6]. If the problem of design of observers for linear systems seems well overcome, this is not the case for nonlinear systems: there is currently no satisfactory global solution.

In this study, extended Kalman filter has been chosen to rebuild the process state. Indeed, this filter is inexpensive in computation time and gives good results for moderate nonlinear systems [5, 7, 8, 26]. It should be noted that as soon as the nonlinearities become too strong or if it is badly initialized, extended Kalman filter is not efficient. In our work, this filter is based on the dynamic simulation of hybrid dynamic systems. PrODHyS simulator [9] provides models, which characterize the process behaviour, especially during the transient states. Thanks to the use of this filter, the monitoring is robust with noises and process uncertainties. It avoids thus false alarms.

The state reconstruction by the extended Kalman filter consists of making the estimation error independent of the uncertainties of the system. A description of this filter and of its implementation can be found in [9, 10].

5.2.2 Residual Generation

Next, residuals $r(t)$ are generated. They result from the comparison between the state vector reconstructed by the observer representing the estimated state $\widehat{X}(t)$, and the state vector $X(t)$ obtained with the reference model:

$$r(t) = \widehat{X}(t) - X(t) \tag{5.1}$$

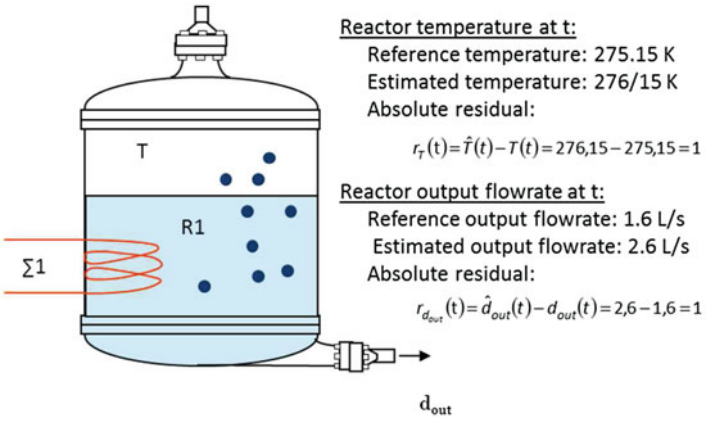

Fig. 5.2 Absolute residual

This residual is called "absolute" residual. Let us illustrate this concept through a simple example (Fig. 5.2). Consider a reactor $R1$ heated by an energy source $\Sigma 1$.

In order to determine the variables representative of the abnormal behaviour, it is necessary to compare the residual of the temperature T and the output flowrate d_{out}. However, although similar in value, these residuals are not dimensionless. To be able to compare them, they must be dimensionless: $r_T(t) = 1\text{K}$ and $r_{d_{\text{out}}}(t) = 1L/s$. For this, a relative residual is defined:

$$r^r(t) = \frac{\widehat{X}(t) - X(t)}{X(t)} \tag{5.2}$$

Then, we obtain the following relative residuals.

$$r^r_T(t) = \frac{\widehat{T}(t) - T(t)}{T(t)} = \frac{276.15 - 275.15}{275.15} = 0.36\%$$

$$r^r_{d_{\text{out}}}(t) = \frac{\widehat{d}_{\text{out}}(t) - d_{\text{out}}(t)}{d_{\text{out}}(t)} = \frac{2.6 - 1.6}{1.6} = 62.5\%$$

It is possible to conclude the output flowrate is a variable representative of the abnormal state, while the temperature is under normal conditions.

5.3 Residual Estimation: Signature Generation

Real-time operation is an important factor in fault detection. Indeed, an early detection of a fault is an asset to avoid its consequences that can be disastrous for a chemical process [2]. In addition, past information can help understand the current behaviour. Then, the observations are collected, according to their availability. Intuitively, we suspect that when the time horizon is large $t \gg 1$, the data of the initial moment will have no influence on the residuals at the date t. So, it is not necessary to collect all the data. An observation window of size T is then defined. The system is observed during the period T. This window is representative of the system state. Its size is a parameter chosen according to system dynamic. Figure 5.3 illustrates the concept of this sliding window.Next, the detection consists of evaluating an instantaneous signature from the residual generation in the first step (Fig. 5.1). We denote this instantaneous signature S. The instantaneous signature (S) is a positive vector of dimension n (the size of the state vector). More specifically, each component of this vector is a positive real which is the result of a threshold test. An element of the signature is thus defined as follows:

$$S_i(t) = \begin{cases} 0 & \text{if} \quad |r_i(t)| \leq \varepsilon_i(t) \\ \alpha_i > 0 & \text{if} \quad |r_i(t)| > \varepsilon_i(t) \end{cases} \quad \text{with} \quad i \in [1;n] \tag{5.3}$$

where α_i is the result of the threshold violation test; $r_i(t)$ is the generated residual in the first part of the diagnosis, $\varepsilon_i(t)$ is the adaptive detection threshold.

S is an instantaneous default signature. A nonzero component of this vector assumes the occurrence of a fault ($S_i(t) = \alpha_i > 0$ with $i \in [1;n]$). A null vector means a priori a normal behaviour of the monitored system ($S_i(t) = 0$ for $i = 1 \ldots n$). This signature vector could be a binary vector: if the residual exceeds the threshold then the signature is equal to 1. Nevertheless, by defining the signature vector in this way, there is a loss of information on the magnitude of the failure: how

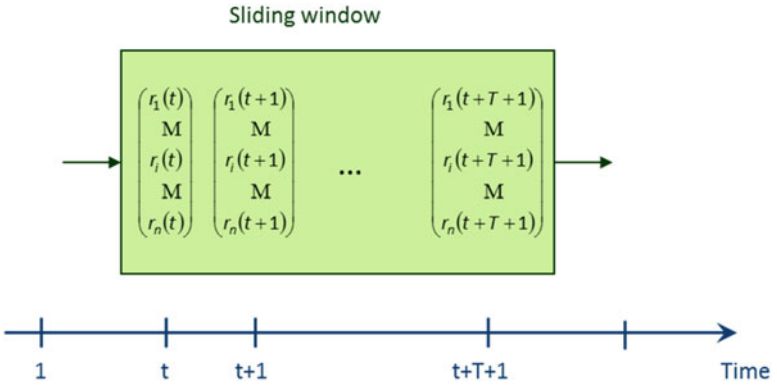

Fig. 5.3 Sliding window

much does it exceed? Is this excess not negligible? By not defining the signature vector as a Boolean, false alarm is thus avoided and the cases of a deviation and of a failure can be differentiated. Moreover, it is hard to detect drift-like fault in early stage. A survey of a drift detection and handling can be found in Sayed-Mouchaweh [11]. In this research work, with the use of a non-binary vector, we have all the necessary information to visualize the effect of a drift on the state vector. Furthermore, thanks to the use of the Kalman filter, it is possible to differentiate drift and model/measurement noises [9].

The instantaneous fault signature $S(t)$ at t is thus a vector function of the residual $r(t)$ and of the detection threshold $\varepsilon(t)$. Each component $S_i(t)$ is defined by the following equation:

$$S_i(t) = \text{Max}\left[\left(|r_i(t)| - \varepsilon_i(t)\right); 0\right] \quad \text{with} \quad i \in [1; n] \tag{5.4}$$

In the previous point, the interest of relative residual is underlined. In the same way, an instantaneous relative fault is defined and it is a function of the relative residual r^r(t), of the detection threshold $\varepsilon(t)$ and X the state vector:

$$S_i^r(t) = \text{Max}\left[\left(\left|r_i^r(t)\right| - \varepsilon_i'(t)\right); 0\right] \quad \text{with} \quad i \in [1; n] \tag{5.5}$$

with $r_i^r(t) = \frac{\widehat{X}_i(t) - X_i(t)}{X_i(t)}$ and $\varepsilon_i'(t) = \frac{\varepsilon_i(t)}{X_i(t)}$.

Finally, it is interesting to normalize these signatures in order to see the predominant variations. Thus, the normalized relative fault signature is defined by the following equation:

$$S_i^{\text{rN}}(t) = \frac{{}_i^r(t)}{\sum\limits_{k=1}^{n} {}_k^r(t)} = \frac{\text{Max}\left[\left(\left|r_i^r(t)\right| - \varepsilon_i'(t)\right); 0\right]}{\sum\limits_{k=1}^{n} \text{Max}\left[\left(\left|r_k^r(t)\right| - \varepsilon_k'(t)\right); 0\right]} \quad \text{with} \quad i \in [1; n] \tag{5.6}$$

Therefore, the sum of all the components of the normalized relative fault signature is 1. This translates the following heuristic: if a residual r_i^r is sensitive to a fault, then the others r_k^r (with $k \neq i$) are not.

5.4 Determination of the Incidence Matrix

Numerous works deal with the distance to the fault signatures or with the structural properties of the incidence matrix in order to have a robustness fault isolation [12–14]. A fault signature is characteristic of a particular residual and a particular fault. This signature is commonly obtained by experiment (or in our case by simulation). The approach consists of evaluating a signature by comparison between the reference model and the experiment or the simulation of the faulty process

(Fig. 5.1). More specifically, each component of this vector is the result of a threshold test (see Eq. (5.6)).

For our approach, we simulate same fault at different times. We generate the characteristic signature of this fault for the p simulations of the faulty process. The goal is then to have an only representation of this fault. Two cases are envisaged:

- The signatures characterize the same state vector. That means that the p simulations have the same importance: their occurrences are equally likely. The characteristic signature corresponds to the centre of gravity of the p signatures obtained by simulation. For complex systems, it is interesting to analyse the data and to determine their main components. Then, an approximate representation of the p simulations is a subspace of small size.
- The signatures don't characterize the same state vector (different number of state variables). It is then necessary to make a canonical analysis. Consider two sets of simulation characterizing the same fault. The first one is represented by the state vector 1 and the second one by the state vector 2. This analysis consists of examining the links existing between these sets. It is based on a Principal Component Analysis decomposition. This theory is described in [15]. Note that if both spaces are confounded, this means that only one of both sets is necessary, since they have the same power of description. Conversely, if these both sets are orthogonal, both sets do not represent the same properties. It is then necessary to consider two different fault signatures characterizing the same fault.

Let's illustrate this initial learning phase. Consider a system characterized by the state vector $[x, y, z]$. A set of simulations is performed by introducing the same fault at different occurrence dates. Let's represent the results on a graph (Fig. 5.4). We thus obtain a pattern characterizing a fault. However, the fault signature may differ according to system state. That is why we can have different theoretical signatures of a fault for different state or we can have an only one (Fig. 5.4).

Once the global incidence matrix is obtained, it is important to rebuild an incidence matrix adapted to the system state (Fig. 5.1). For this, the incidence matrix is reduced: only the present residuals are used in the instantaneous fault signature. Finally, each theoretical fault signature is normalized. Let's do this on a simple example (Fig. 5.5).

5.5 Fault Isolation

The isolation system is represented in Fig. 5.1. It consists of establishing the diagnosis from measured information of the process (instantaneous fault signature) and from information obtained by experiments or by simulation (theoretical fault signatures).

5.5.1 Principle

The columns of the incidence matrix T represent the fault signatures. The notation adopted for the columns of the incidence matrix is the following: $T_{\bullet,j}$ $(j = 1 \ldots m)$. $T_{\bullet,j}$ corresponds to the signature associated with the jth fault f_j. Similarly, each line of the incidence matrix, $T_{i,\bullet}$, represents a signature of the ith residual. Figure 5.6 shows an example of theoretical fault signatures and residual signatures of an incidence matrix.

Our approach is similar to a pattern recognition problem. The form to be classified is the instantaneous normalized relative fault signature S^{rN}, generated in the previous step (Fig. 5.1). It is then necessary to assign this pattern to the existent classes. In our case, each class is represented by a theoretical fault signature $T_{\bullet,j}$ $(j = 1 \ldots m)$.

In the case of fault detection and diagnosis, the instantaneous normalized relative fault signature S^{rN} is therefore compared with the m theoretical fault signatures $T_{\bullet,j}$ $(j = 1 \ldots m)$. The signature S^{rN} transcribes the symptoms of the physical system. The vector $T_{\bullet,j}$ represents the signature of the jth fault. The fineness of the correlation between these both signatures is directly proportional to the occurrence probability of the fault f_j $(j = 1 \ldots m)$. So, if it exists $j \in [1; m]$ such as $S^{rN} \cong T_{\bullet,j}$, then the diagnosis concludes at the occurrence of the fault f_j.

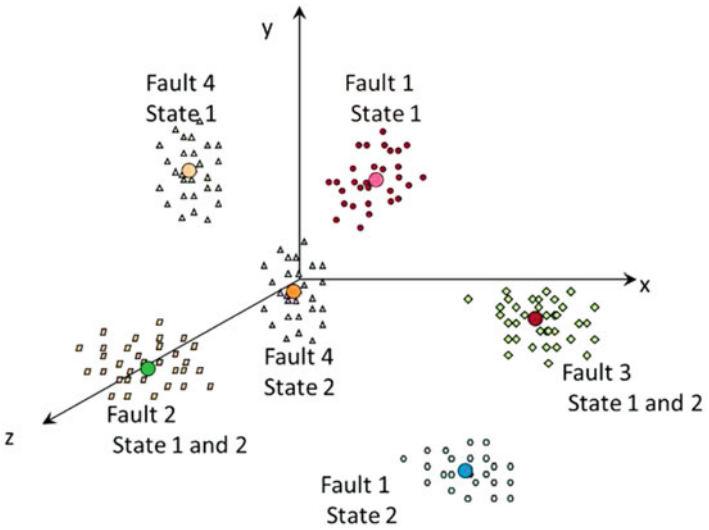

Fig. 5.4 Example of an incidence matrix

Fig. 5.5 Example of the reduction of an incidence matrix

Suppose that the signature obtained is the following:

$$S^{rN} = \begin{pmatrix} 1/2 \\ 1/2 \\ 0 \end{pmatrix} \begin{matrix} r_1 \\ r_3 \\ r_4 \end{matrix}$$

The incidence matrix is the following:

$$T = \begin{array}{c} \\ r_1 \\ r_2 \\ r_3 \\ r_4 \end{array} \begin{array}{c} \begin{matrix} f_1 & f_2 & f_3 & f_4 & f_5 \end{matrix} \\ \begin{pmatrix} 1 & 0 & 0 & 1/3 & 1/3 \\ 0 & 1/2 & 1 & 0 & 1/3 \\ 0 & 0 & 0 & 1/3 & 1/3 \\ 0 & 1/2 & 0 & 1/3 & 0 \end{pmatrix} \end{array}$$

In this example, the residual r_2 doesn't appear in the instantaneous fault signature. It means that the incidence matrix is not adapted. A work on this matrix is therefore necessary. The 2nd row of the incidence matrix is deleted and the resulting fault signatures are normalized:

$$T' = \begin{array}{c} \\ r_1 \\ r_3 \\ r_4 \end{array} \begin{array}{c} \begin{matrix} f_1 & f_2 & f_3 & f_4 & f_5 \end{matrix} \\ \begin{pmatrix} 1 & 0 & 0 & 1/3 & 1/3 \\ 0 & 0 & 0 & 1/3 & 1/3 \\ 0 & 1/2 & 0 & 1/3 & 0 \end{pmatrix} \end{array} \Rightarrow \quad T' = \begin{array}{c} \\ r_1 \\ r_3 \\ r_4 \end{array} \begin{array}{c} \begin{matrix} f_1 & f_2 & f_3 & f_4 & f_5 \end{matrix} \\ \begin{pmatrix} 1 & 0 & 0 & 1/3 & 1/2 \\ 0 & 0 & 0 & 1/3 & 1/2 \\ 0 & 1 & 0 & 1/3 & 0 \end{pmatrix} \end{array}$$

Note that the fault f_3 is not isolable here.

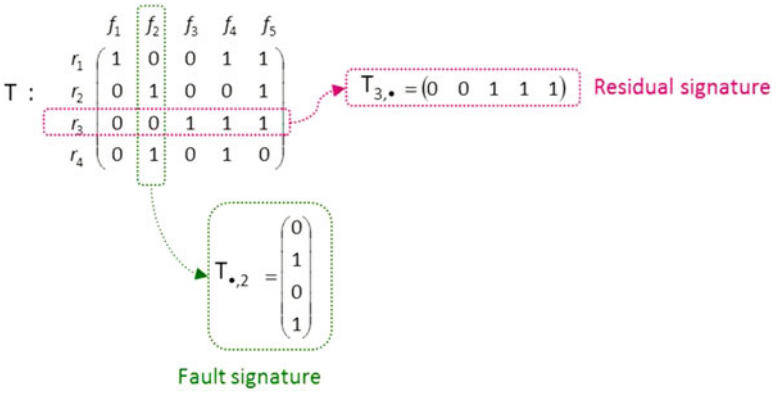

Fig. 5.6 Fault signature and residual signature

In order to compare an instantaneous signature $S^{rN}(t)$ and a particular fault signature $T_{\bullet,j}$, a similarity function or a distance can be used. In our case, the classification is made thanks to a distance in the signature space.

Definition of a Distance Let S be the space of the instantaneous normalized relative signatures and T the bounded space of the theoretical fault signatures (card $(T) = m$, m being the number of considered faults). A distance $S^{rN}(t)$ defines the correlation

symptoms—faults. The distance between an instantaneous signature and a fault signature $T_{\bullet,j}$ is defined by the following expression:

$$D : S \times T \rightarrow [0; 1]$$

$$\left(S^{\mathrm{rN}}(t); T_{\bullet,j}\right) \alpha D_j(t) = D\left(S^{\mathrm{rN}}(t); T_{\bullet,j}\right)$$

The distance D verifies these following properties:
For $X \in S$, $Y \in T$,

1. $D(X, Y) = 0 \Rightarrow X = Y$
2. $D(X, Y) = D(Y, X)$
3. For $Z \in S$, $D(X, Z) \leq D(X, Y) + D(Y, Z)$

Then we define a fault indicator:

Definition of a Fault Indicator A fault indicator $I_j \in [0; 1]$ is specific to the fault f_j with $j = 1 \ldots m$. It represents the occurrence probability of the fault. It is defined by the following relation:

$$I_j(t) = 1 - D_j(t) = 1 - D\left(S^{\mathrm{rN}}(t), T_{\bullet,j}\right) \tag{5.7}$$

According to the property 1 of a distance, $I_j(t) = 0$ means that the fault f_j is not occurring. On the contrary, $I_j(t) = 1$ reflects the fact that the fault f_j is detected and localized.

In general, we will not have these strict equalities, but rather the relation of order: $0 < I_j(t) < 1$.
This relationship triggers an alarm on the fault f_j. If the fault indicator I_j is close to zero, the occurrence of the fault is not proved. On the other hand, if I_j is close to one, then the occurrence of the fault f_j is demonstrated.

5.5.2 Distances

Generally, the distance used is Hamming distance [16, 17]. It is a mathematical distance. It compares two binary vectors B_1 and B_2 of the same size. This distance is equal to the sum of the absolute values of the differences, component by component of the two vectors B_1 and B_2:

$$D^H = \sum_{i=1}^{n} |B_{1i} - B_{2i}| \tag{5.8}$$

Figure 5.7 illustrates the calculation of the Hamming distance between two binary vectors B_1 and B_2. In this example, the Hamming distance is equal to 1.

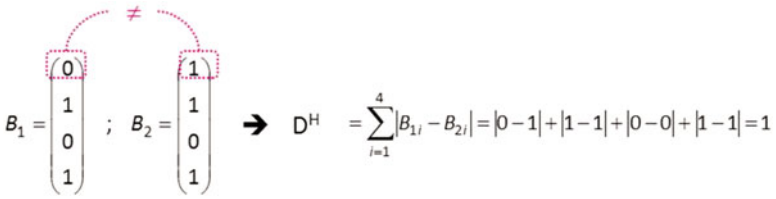

Fig. 5.7 Example of a calculation of Hamming distance

That means that only one component is different between both vectors.In order to standardize this distance for all signatures, the relative Hamming distance has been defined [18]. This distance between two binary vectors B_1 and B_2 is defined by the following expression [19]:

$$D^{\mathrm{Hr}}(t) = \frac{\sum_{i=1}^{n} |B_{1i} - B_{2i}|}{n} \tag{5.9}$$

In the previous section, we underline the interest to work in the continuous space [0;1]. Equation (5.8) can be generalized to non-binary vectors: in this case the distance is called *Manhattan distance*. In the same way, we generalize Eq. (5.9) to the non-binary case and thus define a new distance called: relative Manhattan distance [1, 9, 10]. The demonstration of this definition can be found in [10].

Definition of Relative Manhattan Distance Let S be the space of the instantaneous normalized relative signatures and T the bounded space of the theoretical fault signatures (card $(T) = m$, m being the number of considered faults). The relative Manhattan distance between an instantaneous signature $S^{\mathrm{rN}}(t)$ and a particular fault signature $T_{\bullet j}$ (both of size n) is defined by the following relation:

$$D_j^{\mathrm{Mr}}(t) = \frac{\sum_{i=1}^{n} \left| S_i^{\mathrm{rN}}(t) - T_{ij} \right|}{n} \tag{5.10}$$

One of the major problems of FDI systems is their ability to detect the occurrence of multiple faults and to localize them. Indeed, the theoretical signatures characterize a particular fault. However, the occurrence of multiple fault is represented by a new fault signature [20]. This signature is obtained by combining the theoretical fault signatures [19]. This is illustrated in Fig. 5.8.

Taking into account all the linear combinations of the theoretical signatures is not a satisfactory solution because of the combinatory explosion. It is therefore necessary to use a method which avoids the combination tests. Thus, Theillol et al. [18] have defined a modified Hamming indicator, which only takes into account the nonzero elements of the theoretical fault signature in the comparison:

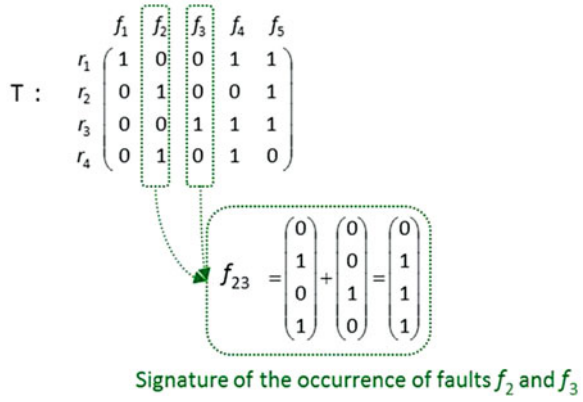

Fig. 5.8 Signature of multiple faults

$$D_j^{\mathrm{Ha}}(t) = \frac{\sum_{i=1}^{n} \left| S_i^{\mathrm{rN}}(t) - T_{ij} \right| \cdot T_{ij}}{n'} \tag{5.11}$$

with n' the number of nonzero elements of the theoretical fault signature $T_{\bullet j}$.We generalize this distance to the non-binary case by defining the improved Manhattan distance D^{Ma} [10]:

$$D_j^{\mathrm{Ma}}(t) = \frac{\sum_{i=1}^{n} \left| S_i^{\mathrm{rN}}(t) \times m' - T_{ij} \times n' \right| \cdot T_{ij}}{n'} \tag{5.12}$$

with n' the number of nonzero elements of the theoretical fault signature $T_{\bullet j}$., m' the number of nonzero elements of the instantaneous fault signature S^{rN}.

Note
Improved Hamming and Manhattan distances are not mathematical distances [10]. Nevertheless, these indicators are called "distance", since these both indicators allow to make a comparison between the instantaneous signature S^{rN} and a particular fault signature $T_{\bullet j}$ in terms of similitude of abnormal symptoms.

Let's apply the relative and improved Manhattan signatures to a concrete example. Consider the case where the faults f_1 and f_2 take place simultaneously. The instantaneous signature vector and the incidence matrix are shown in Fig. 5.9. These distances (Eqs. (5.10) and (5.12)) and the corresponding fault indicators (Eq. (5.7)) are calculated.

In this example, the calculation of the relative Manhattan fault indicators does not allow us to conclude. The instantaneous fault signature does not correspond to any theoretical fault signatures. The improved Manhattan distance is based on the idea of finding in the instantaneous fault signature only the significant symptoms

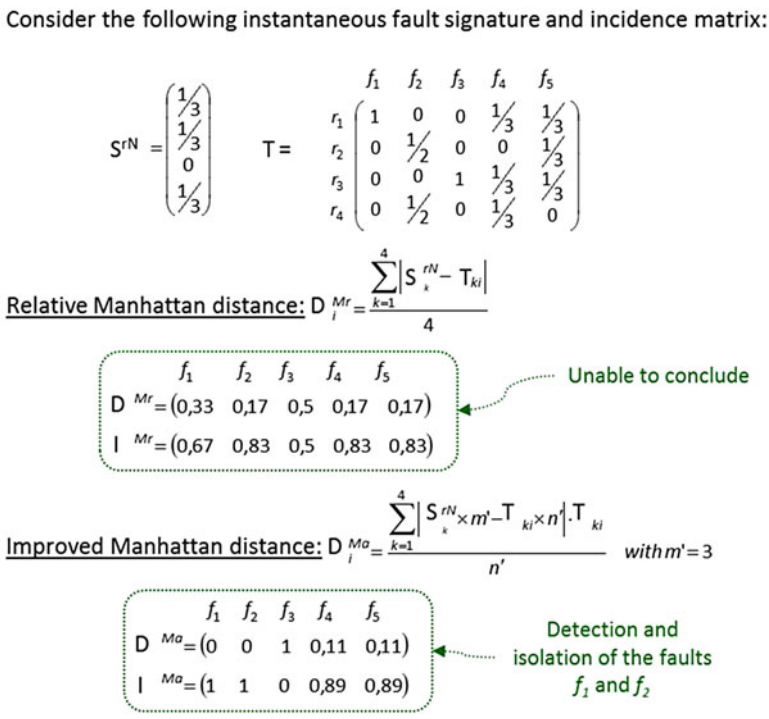

Fig. 5.9 Example of Manhattan distances and corresponding fault indicators

of faults (i.e. the nonzero elements). With the improved Manhattan indicator, both faults f_1 and f_2 are detected and isolated.

5.5.3 Decision Making

The generated fault indicators are then transmitted to the decision step (Fig. 5.1). This step consists of the discrimination of the most probable fault. Since both distances are defined in the space interval [0;1], the fault indicators are defined as the complement to 1 of these distances. An indicator can be viewed as the probability of the occurrence of a particular fault. These indicators follow a reduced centred normal law $\aleph(\mu, \sigma)$. This distribution is shown in Fig. 5.10.This is confirmed by the well-known statistical test of Shapiro-Wilk [21, 27]. This test is used to verify normality. According to the test value, we can accept or reject the hypothesis that the corresponding distribution is normal. The Shapiro-Wilk W test is the most widely used normality test because it is a powerful test compared to many alternative tests [15].

The generated fault indicators are exploited to take a diagnosis of the system. To make this decision, we formulated two postulates:

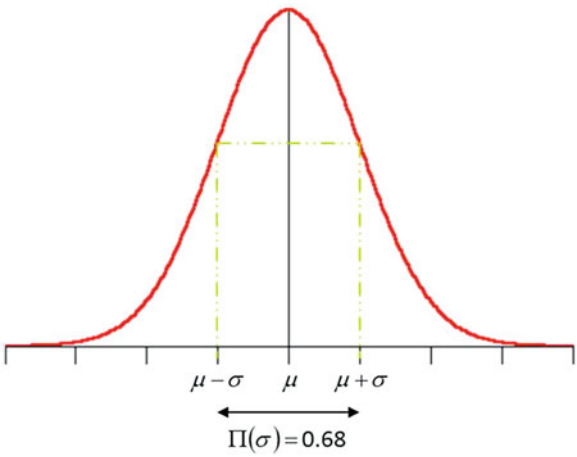

Fig. 5.10 Reduced centred normal law $\aleph(\mu, \sigma)$

- A minimum value of the indicator, for which the fault can be considered, is defined. This threshold is equal to 0.68 and corresponds to the probability at the standard deviation. This allows us to define a limit threshold corresponding to the probability at the standard deviation, i.e. less than 0.68. Thus, the presence of a fault is not valid if its indicator is less than 0.68.
- Then, in order to limit the choice of possible faults, the following hypothesis is put forward: the number of faults, which can simultaneously take place, is limited to three.

5.6 Monitoring of a Complex Chemical Process

In this example, the case study deals with a variant of a chemical process described in [22]. The process is described in Fig. 5.11. The purpose of this installation is to produce and package a product P whose molar purity must be equal to 98%. The reaction considered is an endothermic balanced reaction, whose reaction is the following:

$$R1 + R2 \leftrightarrow P \tag{5.13}$$

In order to maximize the conversion rate of the reaction without penalizing the cycle time of the process, the reaction is stopped as soon as the molar composition of product P reaches the value of 0.8. Moreover, the reaction (R) speed increases with temperature T. The selected temperature for the reaction must guarantee a rapid reaction and maintain the components in the liquid state. A temperature of 383 K satisfies these two constraints. Discrete controller commands the valves (open valve/close valve).

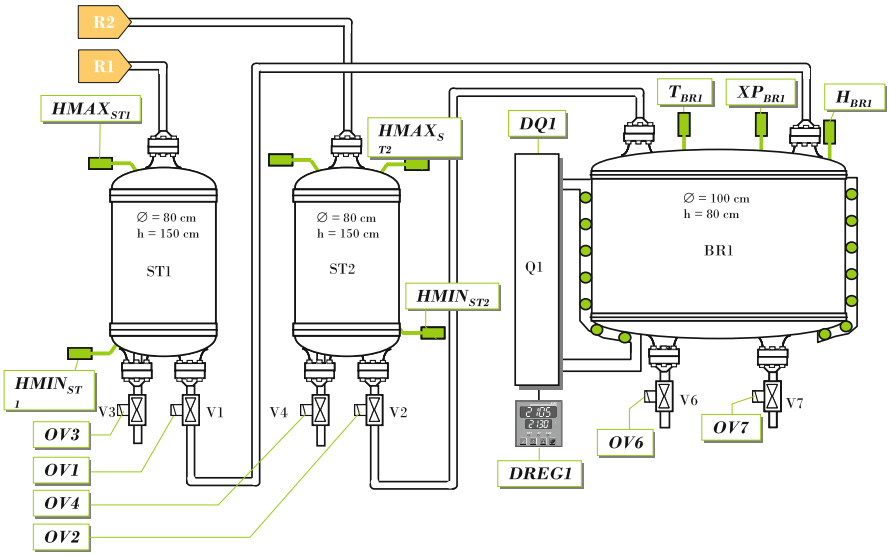

Fig. 5.11 Process flowsheet [22]

The production of P according to the reaction (5.13) in the reactor BR1 involves the following steps:

- Introduction in the reactor with $n/2$ moles of product $R1$,
- Preheating to 383 K,
- Introduction of $n/2$ moles of product $R2$ in the reactor with a temperature control with the set point 383 K,
- Reaction until the product composition P reaches the value of 0.8.

5.6.1 Simulation of the Reference Model

The models used in this simulation take into account global and partial material balances, energy balance, liquid/vapor equilibria, reaction rates, and hydraulic phenomena. Indeed, except the pipes with a pump, the transfers between tanks are carried out by gravity. This implies that the outlet flows of the tanks are a function of the hydraulic pressure and of the liquid level in the source tanks. The transfer times therefore depend on the time evolution of the system state. The simulation is made with the hybrid dynamic simulator PrODHyS. The reader can find more information about PrODHyS in [23]. Figure 5.12 illustrates the time evolution of the composition in the reactor.

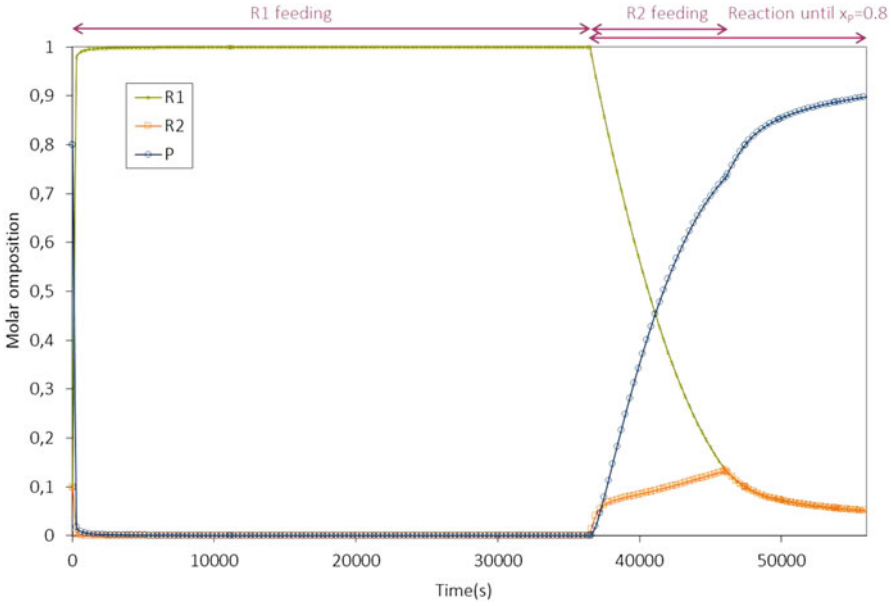

Fig. 5.12 Time evolution of the composition in the reactor

5.6.2 Detection

The proposed approach is illustrated using a chemical process. The fault studied concerns a degradation: the flow rate in valve $V2$ is degraded. That means that valve $V2$ is blocked off partially. It is very interesting to be able to detect and diagnosis a drift in order to avoid the failure [24]. We can find in literature numerous works dealing with this problem [11] .

For this case study, 17 signatures related to a physical quantity are considered:

- The signature s_1 represents the flow rate in the valve $V1$,
- The signature s_2 represents the flow rate in the valve $V2$,
- The signature s_3 represents the $R1$ composition in the tank ST1,
- The signature s_4 represents the $R2$ composition in the tank ST1,
- The signature s_5 represents the P composition in the tank ST1,
- The signature s_6 represents the liquid retention in the tank ST1,
- The signature s_7 represents the $R1$ composition in the tank ST2,
- The signature s_8 represents the $R2$ composition in the tank ST2,
- The signature s_9 represents the P composition in the tank ST2,
- The signature s_{10} represents the liquid retention in the tank ST2,
- The signature s_{11} represents the liquid level in the tank BR1,
- The signature s_{12} represents the $R1$ composition in the tank BR1,
- The signature s_{13} represents the $R2$ composition in the tank BR1,

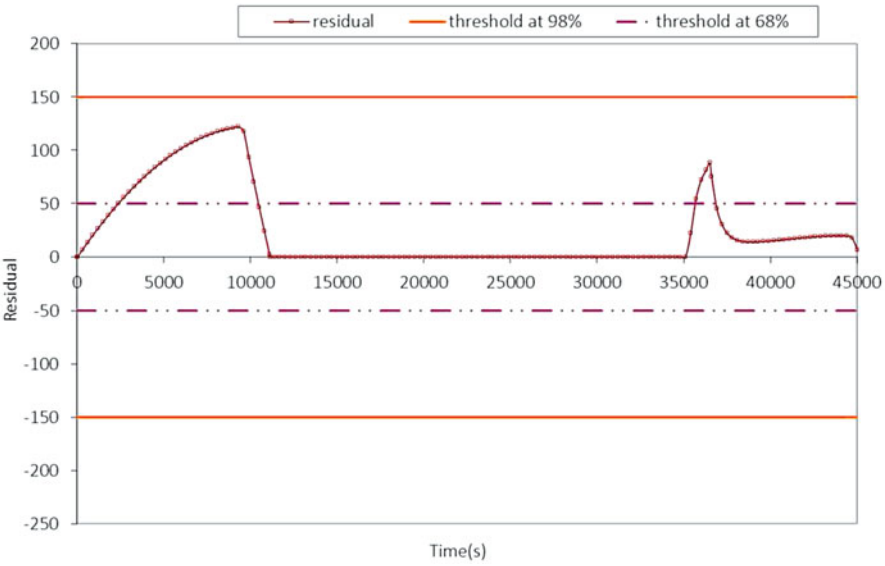

Fig. 5.13 Detection of a drift

- The signature s_{14} represents the P composition in the tank BR1,
- The signature s_{15} represents the temperature in the tank BR1,
- The signature s_{16} represents the liquid retention in the tank ST1,
- And the signature s_{17} represents the heat provided by the power supply of the tank BR1.

Figure 5.13 illustrates the detection step. The residual of the liquid retention for the reactor BR1 is presented. A statistical analysis estimates the prediction errors of the Kalman filter and determines a limit threshold of 150 moles. This threshold corresponds, according to the normal law, to a probability of 98%: there is a probability of 98% that the behaviour is normal in this interval. The obtained residual remains in this confidence interval. That means that this threshold (98%) is not adapted to detect degradation. The threshold must be changed for that and must be lower than this one. A compromise is made to avoid false alarms. For this goal, the same postulate as the fault indicators is formulated: the threshold is lower to a probability of 68% (Fig. 5.10): the new threshold is then obtained at 50 moles. From $t = 2400$ s, the residual is out of the normal operating area. The diagnosis is launched at $t = 3000$ s.

The residual vector is then evaluated and the corresponding instantaneous fault signature is obtained:

5.6.3 Diagnosis

The considered faults in this example are chosen according to a risk assessment study and lessons to learn from accident:

- Fault 1 corresponds to a fault on the power supply of the reactor BR1: the latter supplies a degraded amount of energy.
- Similarly, fault 2 represents a fault in the cooling system of the reactor BR1 which provides a degraded amount of energy.
- Fault 3 is a composition fault on the tank ST1, which normally contains the pure component $R1$. Here, traces of component $R2$ are found in this tank.
- Fault 4 characterizes the same fault but this time there are traces of the constituent P.
- The same type of fault is also considered on the tank ST2 which normally contains the pure component $R2$. Thus, fault 5 represents the fact that component $R1$ exists in tank ST1.
- Fault 6 is the same fault but with component P.
- Fault 7 represents a fault in the reactor power supply which is not at the right temperature.
- Next, actuator faults are considered with the fault 8 corresponding to the blocking of the valve $V1$ in the open position,
- And with the fault 9 corresponding to a degraded state of the valve $V1$: the flow rate of this valve is degraded.
- The fault 10 is identical to the fault 8 but for the valve $V2$.
- Similarly, fault 11 is the same fault as fault 9 but applies to valve $V2$.

The incidence matrix contains all the theoretical fault signatures. An off-line Monte Carlo simulation provides the theoretical signatures. It consists of simulating a fault with different occurrence date. The parameter of the faults change for each simulation and the noises are simulated. For example, consider the fault 9. The flow rate of valve $V1$ is degraded. The valve is blocked off partially due to fooling. The value of the rate of fooling changes. This matrix is rebuilt on-line to match the state vector. This stage has been developed in point 4.

The instantaneous fault signature (Table 5.1) is compared with the incidence matrix by calculating the relative fault indicators for the relative Manhattan distances (Eq. (5.10)) and the improved one (Eq. (5.12)). The obtained indicators are presented in Table 5.2.

Table 5.1 Instantaneous fault signature

s_1	0.21775356	s_7	0	s_{13}	0.16505573
s_2	0	s_8	0	s_{14}	0.16505354
s_3	0	s_9	0	s_{15}	0
s_4	0	s_{10}	0	s_{16}	0.21909804
s_5	0	s_{11}	0.21952267	s_{17}	0
s_6	0.01182547	s_{12}	0		

Table 5.2 Relative and improved Manhattan indicators

	Relative Manhattan indicator	Improved Manhattan indicator
Fault 1	0.92118933	0.84052179
Fault 2	0.92118933	0.86669003
Fault 3	0.90196728	0.15177246
Fault 4	0.90277453	0.19006373
Fault 5	0.88238145	0.0003779
Fault 6	0.88236707	0.00018733
Fault 7	0.92118933	0.86669003
Fault 8	0.92335219	0.67944269
Fault 9	0.98670897	0.95493963
Fault 10	0.92383701	0.84716655
Fault 11	0.99785443	0.99547681

The values 0.68 of the fault indicators do not allow us to avoid faults since all the values are greater than 0.68. On the other hand, the improved fault indicator makes it possible to eliminate faults 3, 5, 6 and 8. We therefore have 6 possible faults. We then use the second hypothesis that we formulated (see point 5.3): there can be no more than three simultaneous faults. Thus, only the indicators with the highest values are kept:

- Fault 11 with a rate of more than 99%,
- Fault 9 with a 95% rate,
- And faults 2 and 7 which have indicator values equal to 98.7%.

By combining the results of both indicators, it is found that fault 11 is in both cases with a rate of more than 99%, and in particular the fault which provides the maximum indicators. We can therefore conclude on the most probable cause of the failure: fault 11, which represents the degraded state of valve $V2$ (the flow rate is lower than the normal one).

The value of the residual then reveals the magnitude of the deviation, i.e. about 0.1. A parametric estimate here would be profitable in order to more precisely determine the opening coefficient of the valve. However, in view of the results, the system is in degraded mode. It may be considered to leave it in this state. In this case, it is interesting to take this degradation into account in the reference model. Finally, we can conclude that the SimAEM methodology is able to detect and diagnose degradation.

5.7 Conclusion

This chapter presents a model-based approach and this methodology is illustrated with the simulation of a complex chemical process. The feasibility of using the simulation as a tool for fault detection is described. The method developed in this study relies on the hybrid dynamic simulator (PrODHyS). The fault detection

and diagnosis approach, developed here, is a general method for the detection and isolation of occurrence of a fault. Besides, this approach allows the detection of numerous types of fault and has the ability to detect and isolate simultaneous faults [1]. The works in progress aim at defining a recovery solution following the diagnosis of fault. For this, the results of signatures will be exploited in order to generate qualitative information. As shown by the example, it is possible to distinguish a simple degradation from a failure. Finally, dynamic simulation of faulty processes is a real asset for safety studies. It makes it possible to analysis the drifts to evaluate their dynamic and their magnitude and thus to define the required safety barriers. Moreover, the simulation results provide predictive information to validate the nature and the sizing of barriers.

References

1. Olivier-Maget, N., Hétreux, G., Le Lann, J. M., & Le Lann, M. V. (2009). Model-based fault diagnosis for hybrid systems: Application on chemical processes. *Computers & Chemical Engineering, 33*(10), 1617–1630.
2. Venkatasubramanian, V., Rengaswamy, R., Yin, K., & Kavuri, S. N. (2003). A review of process fault detection and diagnosis. *Computers & Chemical Engineering, 27*, 293–346.
3. De Kleer, J. (1986). An assumption-based TMS. *Artificial Intelligence, 28*, 127–162.
4. Birouche, A. (2006). *Contribution sur la synthèse d'observateurs pour les systèmes dynamiques hybrides*. Thèse de doctorat, Institut National Polytechnique de Lorraine, Nancy, France.
5. Ding, S. X. (2014). Data-driven design of monitoring and diagnosis systems for dynamic processes: A review of subspace technique based schemes and some recent results. *Journal of Process Control, 24*(2), 431–449.
6. Clark, R. N., Fosth, D. C., & Walton, V. M. (1975). Detection instrument malfunctions in control systems. *IEEE Transactions on Aerospace and Electronic Systems, AES-11*, 465–473.
7. Jazwinski, A. H. (1970). *Stochastic processes and filtering theory*, *Mathematics in Science and Engineering* (Vol. 64). New York: Academic Press.
8. Reif, K., & Unbehauen, R. (1999). The extended Kalman filter as an exponential observer for nonlinear systems. *IEEE Transactions on Signal Processing, 47*(8), 2324–2328.
9. Olivier-Maget, N., Hétreux, G., Le Lann, J. M., & Le Lann, M. V. (2009). Dynamic state reconciliation and model-based fault detection for chemical processes. *Asia Pacific Journal of Chemical Engineering, 4*(6), 929–941.
10. Olivier-Maget, N. (2008). *Surveillance des systèmes dynamiques hybrides: Application aux procédés*. Thèse de doctorat, Université de Toulouse, France.
11. Sayed-Mouchaweh, M. (2016). *Learning from data streams in dynamic environments*, *Springer briefs in electrical and computer engineering* (p. 75). Cham: Springer. ISBN: 978-3-319-25665-8.
12. Chin, H., & Danai, K. (1991). A method of fault signature extraction for improved diagnosis. In *IEEE ACC Conference*, Boston, USA.
13. Fang, C. Z., & Ge, W. (1998). Failure isolation in linear systems. In *IMACS 12th world congress*, Paris, France, pp. 442–446.
14. Gertler, J., & Singer, D. (1990). A new structural framework for parity equation based failure detection and isolation. *Automatica, 26*(2), 381–388.
15. Saporta, G. (1990). *Probabilités, analyse des données et statistique*. Paris: Éditions Technip.
16. Cassar, J. P., Litwak, R.-G., Cocquempot, V., & Staroswiecki, M. (1994). Approche structurelle de la conception de systèmes de surveillance pour les procédés industriels. *Diagnostic et Sûreté de Fonctionnement, 4*(2), 179–202.
17. Kaufmann, A. (1977). *Introduction à la théorie des sous-ensembles flous à l'usage des ingénieurs*. Tomes I et II, Masson.

18. Theillol, D., Weber, P., Ghetie, M., & Noura, H. (1995). A hierarchical fault diagnosis method using a decision support system applied to a chemical plant. In *International Conference on Systems, Man, and Cybernetics*, Canada.
19. Ripoll, P. (1999). *Conception d'un système de diagnostic flou appliqué au moteur automobile*. Thèse de doctorat, Université de Savoie, France.
20. Koscielny, J. M. (1993). Method of fault isolation for industrial processes. *Diagnostic et Sûreté de Fonctionnement, 3*(2), 205–220.
21. Olivier-Maget, N., & Hétreux, G. (2016). Fault detection and isolation for industrial risk prevention. *Journal Européen des Systèmes Automatisés, 49*(4-5), 537–557.
22. Joglekar, G. S., & Reklaitis, G. V. (1985). A simulator for batch and semi-continuous processes. *Computers and Chemical Engineering, 8*(6), 315–327.
23. Olivier-Maget, N., Hétreux, G., Le Lann, J. M., & Le Lann, M. V. (2008). Integration of a failure monitoring within a hybrid dynamic simulation environment. *Chemical Engineering and Processing: Process Intensification, 47*(11), 1942–1952.
24. Toubakh, H., & Sayed-Mouchaweh, M. (2016). Hybrid dynamic classifier for drift-like fault diagnosis in a class of hybrid dynamic systems: Application to wind turbine converters. *Neurocomputing, 171*, 1496–1516.
25. Einicke, G. A., & White, L. B. (1999). Robust extended Kalman filtering. *IEEE Transactions on Signal Processing, 47*(9), 2596–2599.
26. De Kleer, J., & Williams, B. C. (1987). Diagnosing multiple faults. *Artificial Intelligence, 32*, 97–130.
27. Shapiro, S. S., & Wilk, M. B. (1965). An analysis of variance test for normality (complete samples). *Biometrika, 52*(3-4), 591–611.